Available online at www.sciencedirect.com
ScienceDirect
Energy Reports 8 (2022) 359–364
www.elsevier.com/locate/egyr

The 8th International Conference on Energy and Environment Research ICEER 2021, 13–17 September

Offshore wind resource mapping in Cambodia: Sensitivity assessment of the weather research and forecasting model

Soklin Tuy[a], Han Soo Lee[b,*], Karodine Chreng[a]

[a] *Department of Development Technology, Graduate School for International Development and Cooperation (IDEC), Hiroshima University, 1-5-1 Kagamiyama Higashi-Hiroshima, Hiroshima 739-8529, Japan*

[b] *Transdisciplinary Science and Engineering Program, Graduate School of Advanced Science and Engineering, Hiroshima University, 1-5-1 Kagamiyama, Higashi-Hiroshima, Hiroshima 738-8529, Japan*

Received 20 December 2021; accepted 11 January 2022
Available online 2 February 2022

Abstract

The objective of this paper is to assess the sensitivity of the weather research and forecasting (WRF) to three important parameters: nesting with nudging options, planetary boundary layer (PBL) options, and nudged variable options for Cambodian territory. Three tests are set up and carried out, and each of the test, intended for each parameter, is comprised of several experiments. All experiments are simulated for the same period of 15-day. Then the outputs of the WRF model are validated against measured wind data from four meteorological stations at 10 m above the ground level. The results show that the WRF is unlikely influenced by the nesting choices but more sensitive to the PBL options for wind speed simulation. In term of wind direction, the model is insensitive to any of the tested parameters. Through statistical and graphical analyses, the best experiments are found to be the two-way nesting with gridded nudging for nesting with nudging options, MYNN2.5 scheme for PBL options, and nudged wind components for nudged variable. With these optimal configurations, the model is then applied for simulations of higher vertical-level wind and for mapping the offshore wind resource in Cambodia. The offshore winds at 80 and 100 m above sea-level are found to be around 5–7 m/s over Cambodian EEZ.

Peer-review under responsibility of the scientific committee of the The 8th International Conference on Energy and Environment Research, ICEER, 2021.

Keywords: Nesting; Nudging; Offshore wind; Planetary boundary layer; Weather research and forecasting; Renewable energy

1. Introduction

Cambodia, a country in Southeast Asia, has recently allowed the integration of renewable energy into its national grid to reduce the reliance on fossil fuels and hydro power. Beside high potential in the solar source, Cambodia has not realized its offshore wind power resource yet despite a few studies on the onshore wind potential assessment

* Corresponding author.
E-mail address: leehs@hiroshima-u.ac.jp (H.S. Lee).

https://doi.org/10.1016/j.egyr.2022.01.065

Peer-review under responsibility of the scientific committee of the The 8th International Conference on Energy and Environment Research, ICEER, 2021.

such as [1–3]. Due to unavailability of offshore wind measurement in Cambodian sea, the study on offshore wind potential is viable with numerical weather predictions (NWPs).

The well-performed NWP for evaluating wind resource has been claimed to be the WRF [4–6]. Carvalho et al. [7] suggested that simulated results could be much improved by calibrating the model for appropriate physic and numerical options for studied areas. Similarly, many works have investigated the model's sensitivity, and their findings can be summarized as following: PBL schemes together with surface layer schemes have a strong impact on the model; shorter initialization and higher-resolution domains can improve the output accuracy; driving lateral and boundary condition data types slightly affect the model performance; 1-way or 2-way nesting option caused no changes to the results [7–11]. Moreover, the previous studies on nudging methods have provided several recommendations as following: long simulations should be run with enabled nudging options above PBL levels; gridded nudging without interior nudging could improve consistency and accuracy; the spectral nudging works well on precipitation downscaling whereas analysis nudging outperforms on simulating 10 m wind speed, 2 m relative humidity, and air humidity [8,12–14]. However, Mai et al. [15] noted that more research should be done due to the appropriate nudging option varying with regard to the studied areas and layers.

With these prior findings, PBL choice is a site-specific and key configuration for a near-surface wind simulation. The nudging options are also site-specific. Moreover, it is still difficult to locate a study evaluating the effect of all nudged variable combinations. Therefore, in this work, the WRF sensitivity to these three parameter options is examined for Cambodian territory for the purpose of offshore wind resource estimation.

2. Materials and method

2.1. In-situ data

Provided by the Department of Meteorology, Ministry of Water Resource and Meteorology, the wind data observed by four onshore automatic weather stations (AWSs), namely Kampot station (KP), Koh Kong station (KK), Kampong Speu station (KPS), and Takeo station (TK), at the 10 m above ground level (AGL) were retrieved for two years from 01 January 2018 to 31 December 2019. All data were recorded hourly, and a quality check was done with boxplots. Missing data are removed from analyses. The locations and details of the AWS are shown in Fig. 1 and Table 1.

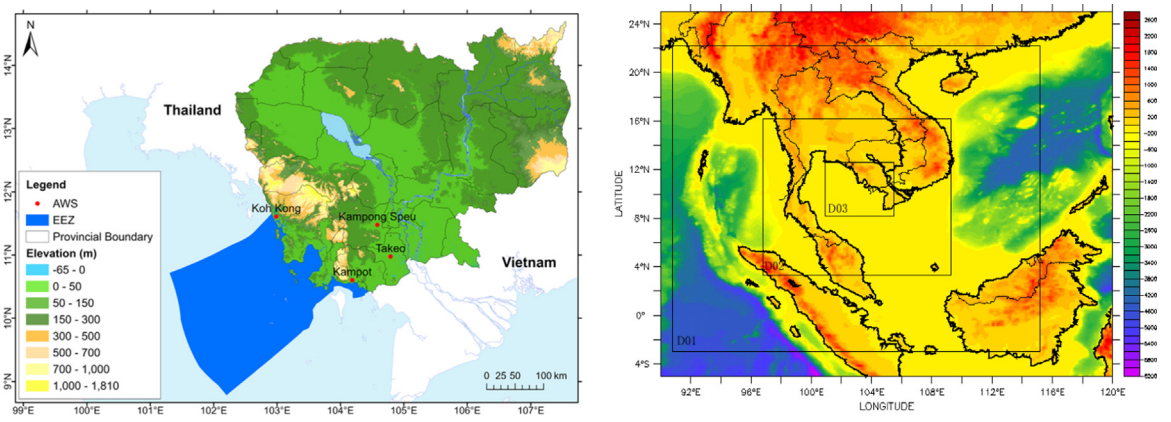

Fig. 1. A map of Cambodia along with the exclusive economic zone (EEZ) and onshore AWS in Kampot, Koh Kong, Kampong Speu, and Takeo provinces (left), and three domains setup for the WRF simulations (right).

2.2. The WRF model design

Three domains are created with a horizontal grid size of 15 km, 5 km, and 1.66 km (Fig. 1). The center of the domains is at 9.8741°N latitudes and 102.9705°E longitudes. For an initial run, the model physic configuration is adopted from Doan et al. [16] with a modification to a cumulus scheme as in Table 2.

Table 1. Overall information of AWSs and elevation differences between the default USGS GTOPO30s topographical data for WRF and the 30m-gridded SRTM elevation dataset.

AWS	Coordinates (Lat (°N), Lon (°E))	Elevation (m) above sea level	Province	Distance from the sea (km)	Elevation difference (m) (GTOPO30 − SRTM)
KP	10.60277, 104.18638	5	coastal	5.3	3.16
KK	11.60833, 102.98805	5	coastal	1.15	15.03
KPS	11.47666, 104.58138	32	inland	110	−0.29
TK	10.97666, 104.79027	9	inland	72	1.41

Table 2. The model setup and initial parameter configuration.

Set-ups/physic parameterizations	Domain 1 (D01)	Domain 2 (D02)	Domain 3 (D03)
Model	WRF-ARW version 3.6.1		
Initial and boundary condition	ERA5 reanalysis, 38 vertical levels		
Vertical layers	38		
Projection	Mercator		
SST update	enabled		
Grid spacing	15 km	5 km	1.66 km
Domain size	180 × 190	277 × 289	298 × 298
PBL scheme	Yonsei University (YSU)		
Surface layer scheme	Revived Monin–Obukhov (Revised MM5)		
Land surface scheme	Unified Noah land surface layer		
Microphysic scheme	WRF Single-Moment 6-class (WSM6)		
Shortwave radiation scheme	Dudhia		
Longwave radiation scheme	RRTMG		
Cumulus scheme	Bett–Miller–Janjic (BMJ)		

Table 3. List of experiments conducted within each test of the WRF sensitivity. The bold indicates the best result of the test (1 = one-way nesting, 2 = two-way nesting, NN = no-nudging, GN = gridded nudging, SN = spectral nudging, V = wind components, T = potential temperature, Q = water vapor mixing ratio, Re. = Revised).

Test	Experiments						
T1	Nesting with nudging options						
	1NN	1GN	1SN	2NN	**2GN**	2SN	
T2	PBL options with respective surface layers						
	YSU	MYJ	QNSE	**MYNN2.5**	ACM2	UW	
	Re. MM5	Janjic Eta	QNSE	**MYNN**	Re. MM5	Re. MM5	
T3	Nudged variable options						
	V	T	Q	VT	VQ	TQ	VTQ

2.3. Sensitivity tests

To investigate the model's sensitivity to the above three parameters, three subsequent tests, namely test 1 (T1) for checking nesting and nudging options, test 2 (T2) for PBL options, and test 3 (T3) for nudged variable options, are carried out. The tests are related because the best results in the prior tests are used in the subsequent ones. Each test is comprised of several experiments as summarized in Table 3. All tests are simulated for the same length of 17 days (from 29 November to 15 December 2019) with the first two days discarded as a spin-up. The simulated outputs of the experiments are validated with the measured wind data from the four AWSs at 10 m AGL. The hourly observed data are collocated with the hourly modeled wind vectors retrieved from D03 at the nearest grid points to the four AWS locations. The best experiment of each test is selected based mainly on Taylor diagrams with statistical indexes. With these optimal configurations, the model is applied for simulations of higher vertical-level wind and for mapping the offshore wind resource in Cambodia.

2.4. Statistical metrics

The model performance is statistically measured by mean bias error (MBE), root-mean-square error (RMSE), the standard deviation error (STDE), and Pearson correlation coefficient (r), defined as follow:

$$MBE = \frac{1}{N}\sum_{i=1}^{N}(P_i - O_i) \tag{1}$$

$$RMSE = \sqrt{\frac{1}{N}\sum_{i=1}^{N}(P_i - O_i)^2} \tag{2}$$

$$STDE = \sqrt{\frac{1}{N}\sum_{i=1}^{N}\left((P_i - O_i) - \frac{1}{N}\sum_{i=1}^{N}(P_i - O_i)\right)^2} = \sqrt{RMSE^2 - MBE^2} \tag{3}$$

$$r = \frac{\sum_{i=1}^{N}\left(O_i - \overline{O}\right)\left(P_i - \overline{P}\right)}{\sqrt{\sum_{i=1}^{N}\left(O_i - \overline{O}\right)^2 \sum_{i=1}^{N}\left(P_i - \overline{P}\right)^2}} \tag{4}$$

where O_i and $\overline{O}$ represent instantaneous and averaged values of the observed wind speed; P_i and $\overline{P}$ represent instantaneous and averaged values of the modeled wind speed; N is the number of samples matched up for the computation.

3. Results and discussion

Six experiments were conducted in T1. The results showed that 2GN was the best experiment as it outperformed other experiments at KP, KPS, and TK (Fig. 2) (only Taylor diagrams for TK were displayed in Fig. 2 due to space limitation). The MBE of this 2GN experiment at the four AWSs ranged from 2.19 m/s – 4.53 m/s, indicating that the WRF outputs overestimated the observed wind speed. Additionally, based on the statistical analyses, it was figured out that one-way and two-way nesting did not seem to affect the model performance. For instance, RMSE of 1GN ranged from 2.27 m/s – 5.43 m/s while RMSE of 2GN was between 2.28 m/s and 5.32 m/s. Rather, the nudging choices showed much influenced on the model simulation of wind speed in T1. These findings were also highlighted by [11,13].

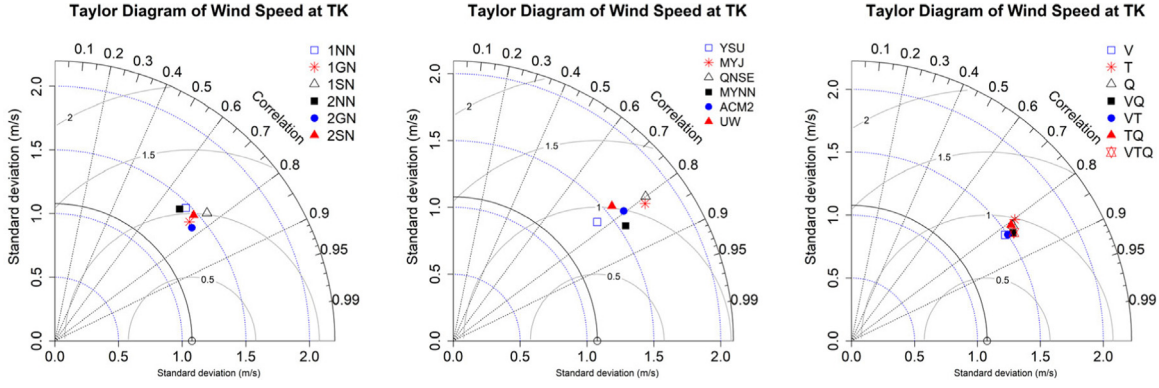

Fig. 2. Taylor diagrams for wind speed at TK, illustrating comparisons among experiments in T1 (left), T2 (centered), and T3 (right).

In T2, the MYNN2.5 PBL scheme was selected for the best experiment because the Taylor diagrams portrayed that it outperformed other schemes at KK, TK and the second-best at KP (Fig. 2). This optimal scheme still widely overpredicted the observed wind speed at all stations (MBE between 1.97 m/s and 3.69 m/s) despite remarkable improvement with respect to the T1. The overprediction may be caused by the model's overestimation tendency

when simulated at very near surface wind (10 m AGL) as reported in [5,9,17]. Furthermore, it is partly attributed to the model's inappropriate representation of the actual topography. The elevation at the four AWS sites from the default GTOPO 30 topographic data for WRF and from the Shuttle Radar Topography Mission (SRTM) data signaled the height differences by stations which corresponded with the errors found in the statistical analyses (Table 1). KP and KK whose elevation differences were high apparently demonstrated the highest errors in wind speed among the four stations. This cause was also emphasized by [17]. The MYJ and QNSE PBL became the worse choices at almost all stations because their wind speed prediction contained the highest overshoots during the daytime. Among seven experiments in T3, the nudged-wind-component experiment (V) marginally led others at KK and TK (Fig. 2). It also became the second-best experiment at KP. According to the results, nudging V was chosen for the optimal configuration for nudged variable option. However, its MBE remained large (1.84 m/s – 3.65 m/s) with little improvement from T2 results. Statistically, nudged T might have the lowest MBE and RMSE. While nudging V seemed to result in the smallest STDE values, nudged VT and VTQ produced the best r values for wind simulation.

In term of wind direction, all experiments of the three tests underestimated the in-situ data at all stations. There was seemingly no noticeable difference among the experiments, but, among the stations, KP had the largest MBE and STDE (>100 degrees). It could mean that neither all tests nor experiments had an influence on the WRF performance in wind direction. Moreover, the wind direction was affected more by the topographical representation in the model than the physic parameterization [18,19].

Based on the results of the sensitivity tests, the final configuration of WRF was later used to simulate offshore wind at two hub heights 80 m and 100 m above sea level (Fig. 3). Over the Cambodian EEZ, the estimated offshore wind at 80 m and 100 m was estimated in the ranges around 5 – 7 m/s. Near the KP, the offshore winds are found to be higher than other regions in the EEZ.

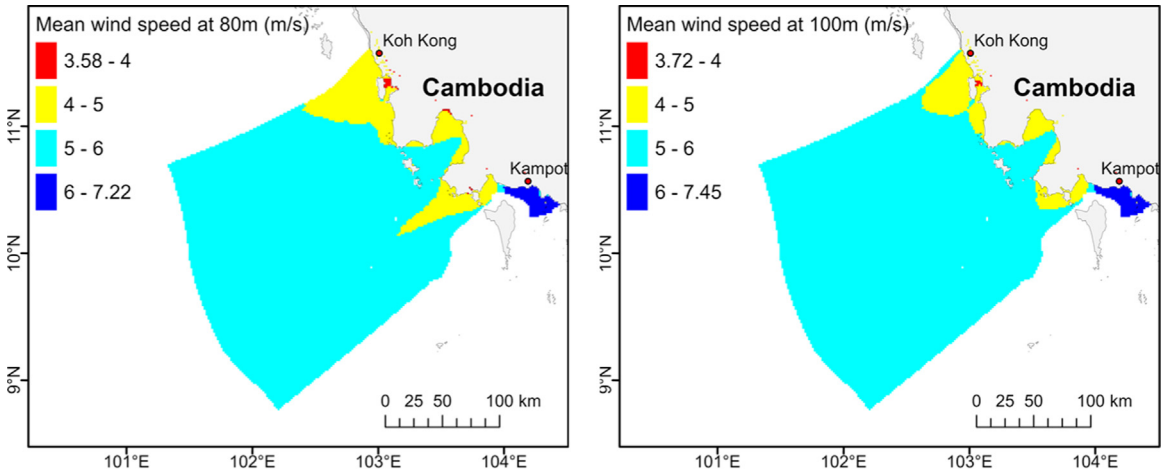

Fig. 3. Annual mean wind speed over Cambodian EEZ at 80 m (left) and 100 m (right) above sea level.

4. Conclusion

In this study, the WRF sensitivity to nesting with nudging options, PBL schemes, and nudged variable options for Cambodia is evaluated. The results show that two-way nesting with gridded nudging, MYNN2.5 scheme, and nudged wind components are the suitable options for the parameters tested in T1, T2, and T3, respectively. Moreover, for wind speed, it is found that the model is likely insensitive to the nesting choices though they are tested along with the nudging options. PBL schemes seem to significantly affect the WRF performance. However, for wind direction, it is not influenced by the choices of the tested parameters but rather sensitive to the topography. Despite overestimation of in-situ wind speed at the four sites at 10 m AGL, the results of WRF simulation can be further used to estimate the offshore wind resources for possible offshore wind power generation in Cambodia.

Declaration of competing interest

The authors declare that they have no known competing financial interests or personal relationships that could have appeared to influence the work reported in this paper.

Acknowledgment

The authors would like to express the gratitude to the Department of Meteorology, Ministry of Water Resource and Meteorology, for the in-situ data at the four AWS sites. These measured data are available upon request.

References

[1] Janjai S, Promsen W, Masiri I, Laksanaboonsong J. Wind resource maps for cambodia. J Sustain Energy Environ 2013;4:159–64.
[2] Promsen W, Janjai S, Tantalechon T. An analysis of wind energy potential of Kampot province, southern Cambodia. Energy Procedia 2014;633–41. http://dx.doi.org/10.1016/j.egypro.2014.07.119.
[3] TrueWind Solutions L. Wind energy resource Atlas of Southeast Asia. Washington, DC: World Bank Group; 2001, (English).
[4] Carvalho D, Rocha A, Gómez-Gesteira M, Silva Santos C. Comparison of reanalyzed, analyzed, satellite-retrieved and NWP modelled winds with buoy data along the Iberian Peninsula coast. Remote Sens Environ 2014;152:480–92. http://dx.doi.org/10.1016/j.rse.2014.07.017.
[5] Salvação N, Guedes Soares C. Wind resource assessment offshore the atlantic iberian coast with the WRF model. Energy 2018;145:276–87. http://dx.doi.org/10.1016/j.energy.2017.12.101.
[6] Lee Han Soo, Yamashita Takao, Hsu John, Ding Fei. Integrated modeling of the dynamic meteorological and sea surface conditions during the passage of Typhoon Morakot. Dyn. Atmos. Ocean. 2013;59:1–23. http://dx.doi.org/10.1016/j.dynatmoce.2012.09.002.
[7] Carvalho D, Rocha A, Gómez-Gesteira M, Santos C. A sensitivity study of the WRF model in wind simulation for an area of high wind energy. Environ Model Softw 2012;33:23–34. http://dx.doi.org/10.1016/j.envsoft.2012.01.019.
[8] Dzebre DEK, Acheampong AA, Ampofo J, Adaramola MS. A sensitivity study of surface wind simulations over coastal Ghana to selected time control and nudging options in the weather research and forecasting model. Heliyon 2019;5:e01385. http://dx.doi.org/10.1016/j.heliyon.2019.e01385.
[9] Gómez-Navarro JJ, Raible CC, Dierer S. Sensitivity of the WRF model to PBL parametrisations and nesting techniques: Evaluation of wind storms over complex terrain. Geosci Model Dev 2015;8:3349–63. http://dx.doi.org/10.5194/gmd-8-3349-2015.
[10] Lo JC-F, Yang Z-L, Pielke RA. Assessment of three dynamical climate downscaling methods using the weather research and forecasting (WRF) model. J Geophys Res 2008;113. http://dx.doi.org/10.1029/2007jd009216.
[11] Witha B, Hahmann AN, Sīle T, Dörenkämper M, Ezber Y, García-Bustamante E, et al. Report on WRF model sensitivity studies and specifications for the mesoscale wind atlas production runs: Deliverable V4.3, NEWA-New European Wind Atlas. 2019, http://dx.doi.org/10.5281/zenodo.2682604.
[12] Bowden JH, Otte TL, Nolte CG, Otte MJ. Examining interior grid nudging techniques using two-way nesting in the WRF model for regional climate modeling. J Clim 2012;25:2805–23. http://dx.doi.org/10.1175/JCLI-D-11-00167.1.
[13] Ma Y, Yang Y, Mai X, Qiu C, Long X, Wang C. Comparison of analysis and spectral nudging techniques for dynamical downscaling with the WRF model over China. Adv Meteorol 2016;2016. http://dx.doi.org/10.1155/2016/4761513.
[14] Vincent CL, Hahmann AN. The impact of grid and spectral nudging on the variance of the near-surface wind speed. J Appl Meteorol Climatol 2015;54:1021–38. http://dx.doi.org/10.1175/JAMC-D-14-0047.1.
[15] Mai X, Ma Y, Yang Y, Li D, Qiu X. Impact of grid nudging parameters on dynamical downscaling during summer over mainland China. Atmosphere 2017;8. http://dx.doi.org/10.3390/atmos8100184.
[16] Doan VQ, Dinh VN, Kusaka H, Cong T, Khan A, Van Toan D, et al. Usability and challenges of offshore wind energy in Vietnam revealed by the regional climate model simulation. Sci Online Lett Atmos 2019;15:113–8. http://dx.doi.org/10.2151/SOLA.2019-021.
[17] Carvalho D, Rocha A, Gómez-Gesteira M, Silva Santos C. WRF wind simulation and wind energy production estimates forced by different reanalyses: Comparison with observed data for Portugal. Appl Energy 2014;117:116–26. http://dx.doi.org/10.1016/j.apenergy.2013.12.001.
[18] Hariprasad KBRR, Srinivas C v, Singh AB, Bhaskara SV, Baskaran R, Venkatraman B. Numerical simulation and intercomparison of boundary layer structure with different PBL schemes in WRF using experimental observations at a tropical site. Atmos Res 2014;145–146:27–44. http://dx.doi.org/10.1016/j.atmosres.2014.03.023.
[19] Santos-Alamillos FJ, Pozo-Vazquez D, Ruiz-arias JA, Fanego-Lara V, Tovar-Pescador J. Analysis of WRF model wind estimate sensitivity to physics parameterization choice and terrain representation in Andalusia (Southern Spain). J Appl Meteorol Climatol 2013;52:1592–609. http://dx.doi.org/10.1175/JAMC-D-12-0204.1.